Nitric Oxide Deligation from Nitrosyl Complexes of Two Transition Metal Porphyrins: A Photokinetic Investigation

Elisabeth A. Morlino and Michael A. J. Rodgers*

Contribution from the Center for Photochemical Sciences, Bowling Green State University, Bowling Green, Ohio 43403

Received July 19, 1996[⊗]

Abstract: The results of an investigation of the ultrafast dynamics of photoinduced deligation in two transition metalloporphyrin−nitrosyl complexes, $TPPFe^{II}NO$ and $TPPCo^{II}NO$, in conjuction with the results of an energy transfer study lead to the conclusion that the difference in the denitrosylation yields ($\phi_{NO} = 0.5$ for $TPPFe^{II}NO$ and $\phi_{NO} = 1.0$ for $TPPCo^{II}NO$) is the result of energy partitioning in the upper excited states of the porphyrin. The energy transfer study yielded the energies of the metal centered states, believed to be of CT(π,d_z^2) nature, and of the localized porphyrin triplet states. The CT states in the two complexes were found to lie at similar energies ($TPPFe^{II}NO$ 8650 cm^{-1} and $TPPCo^{II}NO$ 8900 cm^{-1}); however, the localized porphyrin triplet states were found to be at 16200 cm^{-1} in $TPPFe^{II}NO$ and 14700 cm^{-1} in $TPPCo^{II}NO$. This difference in energies of the respective triplet states facilitates efficient intersystem crossing in the excited state deactivation of $TPPFe^{II}NO$, but does not allow any triplet formation in $TPPCo^{II}NO$. The direct excitation studies revealed that intersystem crossing in $TPPFe^{II}NO$ occurs with a rate constant of 7.3×10^{11} s^{-1} to yield a localized porphyrin triplet state that absorbs maximally at 450 nm. This state then relaxes back to the ground state without the loss of NO. Only those excited states that relax via the CT state result in loss of NO. The direct excitation studies yielded no evidence for intersystem crossing in the deactivation of the electronically excited singlet state of $TPPCo^{II}NO$, hence all of the energy deposited in the initial photoexcitation step results in NO loss. The lifetimes and spectral characteristics of the other excited states involved in deactivation of these transition metalloporphyrin−nitrosyl complexes will be discussed.

Introduction

Nitric oxide (NO) is a diatomic free radical that recently has been found to be a significant biological entity in that it regulates blood pressure, acts as a neurotransmitter, and aids in the immune system's ability to kill intracellular parasites.[1−4] Like the other diatomics O_2 and CO, NO can act as an axial ligand in transition metalloporphyrins (MP). A recent report shows that nitric oxide binds to the heme center in mouse hemoglobin, and the suggestion has been made that this also may be the case in humans.[5] Another report has shown that nitric oxide binds to the ferric-heme prosthetic groups in nitric oxide synthase (NOS), the dimeric enzyme responsible for NO production in humans.[6] This binding, in turn, deactivates the enzyme, thus providing an unusual example of a self-regulating enzyme whose products deactivate itself. The nitrosyl adducts of metalloporphyrins are known to be light sensitive, losing nitric oxide with quantum yields that vary from virtually zero to unity when photons are absorbed by the porphyrin macrocyclic π-system.[7−15] It has been suggested that the identity of the bound metal is one of the most important features in determining the photoinduced deligation yields,[8] although little is known about the factors controlling denitrosylation in these compounds because of (i) the very short time scale on which this process takes place and (ii) the spectroscopic inaccessibility of the internal metal states suspected to be involved. The electronic excited states in these systems are inherently short-lived because the transition metals have empty d-orbitals which can couple to the porphyrin π-orbitals to form states of intermediate energy, thereby facilitating rapid deactivation of the excited porphyrin (π,π*) states.[16,17] A recent communication from this laboratory indicated that the deligation in a protein-free nitrosylmetalloporphyrin occurs on the sub-picosecond time scale from an internal metal charge transfer state.[18]

An intriguing question that generated our interest in this area of photophysics concerns the way in which the incorporated transition metal alters and controls the deactivation dynamics and the deligation quantum efficiencies of the nitrosylmetalloporphyrin (NOMP) system. We have elected to avoid protein-based MPs simply because protein dynamics have been cited[19−24]

* Author to whom correspondence should be addressed.

[⊗] Abstract published in *Advance ACS Abstracts,* November 15, 1996.

(1) Feldman, P. L.; Griffith, O. W.; Stuehr, D. J. *Chem. Eng. News* **1993**, 71, 26.
(2) Karupiah, G.; Xie, Q.; Buller, R. M. L.; Nathan, C.; Duarte, C.; MacMicking, J. D. *Science* **1993**, *261*, 1445.
(3) Lipton, S. L. *Nature* **1993**, *364*, 626.
(4) Edelman, G. M.; Gally, J. A. *Proc. Natl. Acad. Sci. U. S. A.* **1992**, *89*, 11651.
(5) Stamler, J. S.; Jai, L.; Bonaventura, C.; Bonaventura, J. *Nature* **1996**, *380*, 221.
(6) Abu-Soud, H. M.; Wang, J.; Tousseau, D. L.; Fukuto, J. M.; Ignarro, L. J.; Stuehr, D. J. *J. Biol. Chem.* **1995**, *270*, 22997.
(7) Traylor, T. G.; Magde, D.; Marsters, J.; Jongeward, K.; Wu, G. Z.; Walda, K. *J. Am. Chem. Soc.* **1993**, *115*, 4808.
(8) Hoshino, M.; Kogure, M. *J. Phys. Chem.* **1989**, *93*, 5478.
(9) Hoffman, B. M.; Gibson, Q. H. *Proc. Natl. Acad. Sci. U. S. A.* **1978**, *75*, 21.
(10) Gibson, Q. H.; Ainsworth, S. *Nature* **1957**, *180*, 1416.
(11) Gibson, Q. H.; Hoffman, B. M.; Crepeau, R. J. H.; Edelstein, S. J.; Bull, C. *Biochem. Biophys. Res. Commun.* **1974**, *59*, 146.
(12) Hoshino, M.; Ozawa, K.; Seki, H.; Ford, P. C. *J. Am. Chem. Soc.* **1993**, *115*, 9568.
(13) Jongeward, K. A.; Marsters, J. C.; Mitchell, M. J.; Magde, D.; Sherma, V. S. *Biochem. Biophys. Res. Commun.* **1986**, *140*, 962.
(14) Hoshino, M.; Arai, S.; Yamaji, M.; Hama, Y. *J. Phys. Chem.* **1986**, *90*, 2109.
(15) Yamaji, M.; Hama, Y.; Miyazaki, Y.; Hoshino, M. *Inorg. Chem.* **1992**, *31*, 932.
(16) Antipas, A.; Gouterman, M. *J. Am. Chem. Soc.* **1983**, *105*, 4896.
(17) Tait, C. D.; Holten, D.; Gouterman, M. *Chem. Phys. Lett.* **1983**, *100*, 268.
(18) Morlino, E. A.; Walker, L. A., II; Sension, R. J.; Rodgers, M. A. J. *J. Am. Chem. Soc.* **1995**, *117*, 4429.
(19) Rose, E. J.; Hoffman, B. M. *J. Am. Chem. Soc.* **1983**, *105*, 2866.

S0002-7863(96)02510-3 CCC: $12.00

as causing complications in elucidating the core factors that control deligation as well as determining the absolute deligation yields. Except for the previously cited communication from this laboratory, all the previous work done on the protein-free nitrosylmetalloporphyrins has focused on longer time scale studies where the recombination of NO and the free metalloporphyrin has been the issue of concern. However, our recent study on the ultrafast dynamics of the $TPPCo^{II}NO$ system demonstrated that these systems show a richness of photophysical dynamics which deserves investigation since understanding them could well shed light on the processes leading to deligation.[18]

Moreover, in order to gain access to the internal metal states which are thought to be responsible for deligation in nitrosylmetalloporphyrins, an energy transfer study has been employed. Stanford and Hoffman used such a study to examine the nature and energies of the electronic states involved in photodeligation from a carbonylmetalloporphyrin.[25] They showed that the decarbonylation occurs from a state with higher than singlet multiplicity residing no higher than 14300 cm^{-1} in energy. In the present study, the energies of the internal states of the nitrosylmetalloporphyrin system as well as some information concerning their identity are revealed through measurements of energy transfer rate constants with a series of donors of varying triplet energy. An analysis based on the Sandros approach allows energy levels to be determined.[26]

Experimental Section

Materials. Nitrosylcobalt(II) *meso*-tetraphenylporphyrinate was prepared by introduction of NO gas (Liquid Carbonic, CP grade), previously scrubbed of higher oxides by passage through a KOH column, into a nitrogen-saturated solution of $TPPCo^{II}$ (Midcentury Chemicals) in benzene as described in previous publications.[8,18] After the mixture was bubbled for ~20 min, NO-saturated MeOH was added until precipitation of the adduct was complete. The reaction vessel was evacuated and purged with N_2. The resulting precipitate was collected under N_2, dried, and stored under vacuum. The identity of the product was verified by comparison of its UV−visible absorption spectrum to previously published spectra.[8] The new band observed at 1694 cm^{-1} in the infrared absorption spectrum, taken in a KBr pellet, corresponded to the bound NO stretching frequency.[27−29]

Nitrosyliron(II) *meso*-tetraphenylporphyrinate was prepared by the reductive nitrosylation of $TPPFe^{III}Cl$ under conditions previously reported.[30] This involved introduction of NO gas into a nitrogen-saturated chloroform/pyridine solution of $TPPFe^{III}Cl$ (Midcentury Chemicals). After the mixture was bubbled with NO for ~20 min, a NO-saturated MeOH solution was added until precipitation was complete. After the reaction flask was purged with N_2, the resulting precipitate was collected under N_2, dried, and stored under vacuum. The identity of this compound was again verified by comparison of its UV−visible absorption spectrum in benzene to that of the previously published spectrum[8] and the observation of the NO stretching band at 1698 cm^{-1} in an infrared absorption spectrum taken in a KBr pellet.[30] The identity of the product was checked by verifying the Soret and Q-band maxima before each experiment was performed. Since $TPPFe^{II}$-NO appeared to be more air sensitive than the Co(II) analogue, all solutions employing this compound were prepared under a nitrogen atmosphere.

The results presented in this paper were obtained in nitrogen- or argon-saturated benzene (Fluka > 99.5% g.c.) solutions. All the sensitizers employed in this study were either employed in prior studies in this laboratory[31] or used as received from the commercial suppliers. Benzophenone was purchased from Fisher Scientific; phenanthrene, pyrene, acridine, anthracene, 2,2′:5′,2″-terthiophene, perylene, 1,8-diphenyl-1,3,5,7-octatetraene (DPOT), 2,3-benzanthracene (tetracene), pentacene, *trans*-β-carotene, and rubrene were all obtained from Aldrich Chemical Co. SiPC ($(Hex_3SiO)_2$Si-phthalocyanine), GePC ($(OSiEt_3)_2$-Ge-$(OBu)_8$-phthalocyanine), SiNC ($[SiO(i\text{-}C_4H_9)_2n\text{-}C_{18}H_{37}]_2$Si-naphthalocyanine), and SnNC ($[SiO(n\text{-}C_6H_{13})_3]_2$Sn-naphthalocyanine) were all obtained from Professor Malcolm E. Kenney at Case Western Reserve University.

Flash Photolysis. Nanosecond flash photolysis studies were performed using a kinetic spectrophotometric detection system, previously described.[32] Excitation pulses (7 ns) of light were generated: (a) at 355 nm, the third harmonic of a Q-switched Nd:YAG laser (Continuum YAG660, Continuum Surelite I); (b) in the range 420 to 680 nm, from an OPOTEK Magic Prism optical paramagnetic oscillator (OPO) pumped by the third harmonic of the Nd:YAG laser; and (c) at 683 nm, the output of a home-built Raman shifter filled with 100 psi of hydrogen gas and pumped by the second harmonic (532 nm) of a Nd:YAG laser. The combination of these three systems allowed optimal excitation of the sensitizer or of the porphyrin. Typical excitation pulse amplitudes were a few millijoules per pulse. Transients produced were followed temporally and spectrally by a computer-controlled kinetic spectrophotometer, previously reported.[32]

Picosecond flash photolysis experiments were performed employing either 355- or 532-nm pulses (30 ps) of a few millijoules per pulse from an active−passive mode-locked laser system (Continuum YAG571C). Typical pump-probe experiments were carried out using a dual-diode-array detection system (Princeton Instruments ST120), previously described,[33] to monitor the ensuing transients. Kinetic profiles were assembled by recording transient spectra taken at different time delays between the pump and probe paths. All solutions employed in these experiments were flowed to ensure the presentation of a fresh sample to the excitation beam at each shot. The path lengths of the cells varied from 1 cm to 2 mm in order to obtain optimal signals and the solutions were prepared to have an absorbance of 0.7−1.0 at the excitation wavelength in their respective cells.

The femtosecond experiments reported herein were performed at the Chemistry Department at the University of Michigan (Ann Arbor). These experiments employed excitation pulses of 400 or 390 nm light generated by a regeneratively amplified Ti:sapphire laser system, details of which can be found elsewhere.[34] The kinetic profiles of the resulting transients were followed by using an interference filter to select a wavelength of interest from a white light continuum generated by passing the fundamental wavelength through a 1 cm path length cell of flowing ethylene glycol. Data were recorded using a pair of photodiodes to monitor the difference in the absorption changes as a function of delay between the pump and probe beams. The instrument response of the system was measured at 200 fs optimally. All of the kinetic profiles show the instrument response function at the time the data was recorded. The solutions studied were flowed to ensure presentation of a fresh sample to the excitation beam. The samples were prepared to have an absorbance of 1.0 at the excitation wavelength in a 0.5 mm path length cell.

(20) Morris, R. J.; Gibson, Q. H. *J. Biol. Chem.* **1980**, *255*, 8050.
(21) Cornelius, P. A.; Hochstrasser, R. M.; Steele, A. W. *J. Mol. Biol.* **1983**, *163*, 119.
(22) Petrich, J. W.; Martin, J. L. *Chem. Phys.* **1989**, *131*, 31.
(23) Petrich, J. W.; Lambry, J. C.; Kuczera, K.; Darplus, M.; Poyart, C.; Martin, J. L. *Biochemistry* **1991**, *30*, 3975.
(24) Petrich, J. W.; Martin, J. L.; Houde, D.; Poyart, C.; Orszag, A. *Biochemistry* **1987**, *26*, 7914.
(25) Stanford, M. A.; Hoffman, B. M. *J. Am. Chem. Soc.* **1981**, *103*, 4104.
(26) Sandros, K. *Acta. Chem. Scand.* **1964**, *18*, 2355.
(27) Kozuka, M.; Nakamoto, K. *J. Am. Chem. Soc.* **1981**, *103*, 2162.
(28) Scheidt, W. R.; Hoard, J. R. *J. Am. Chem. Soc.* **1973**, *95*, 8281.
(29) Wayland, B. B.; Minkiewicz, J. V.; Abd-Elmageed, M. E. *J. Am. Chem. Soc.* **1974**, *96*, 2795.
(30) Scheidt, W. R.; Frisse, M. E. *J. Am. Chem. Soc.* **1975**, *97*, 17.
(31) (a) Firey, P. A.; Ford, W. E.; Sounik, J. R.; Kenney, M. E.; Rodgers, M. A. J. *J. Am. Chem. Soc.* **1988**, *110*, 7627. (b) Rihter, B. D.; Kenney, M. E.; Ford, W. E.; Rodgers, M. A. J. *J. Am. Chem. Soc.* **1990**, *112*, 8064. (c) Rihter, B. D.; Kenney, M. E.; Ford, W. E.; Rodgers, M. A. J. *J. Am. Chem. Soc.* **1993**, *115*, 8146.
(32) Ford, W. E.; Rodgers, M. A. J. *J. Phys. Chem.* **1994**, *98*, 3822.
(33) Logunov, S. L.; Rodgers, M. A. J. *J. Phys. Chem.* **1992**, *96*, 2915.
(34) Squier, J.; Salin, F.; Mourou, G.; Harter, D. *Opt. Lett.* **1991**, *16*, 324.

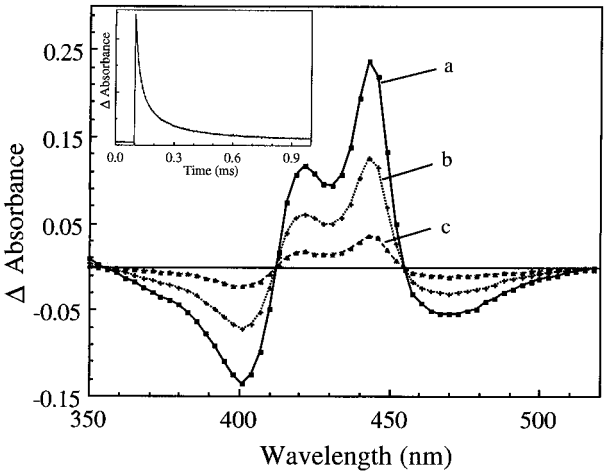

Figure 1. Transient absorption difference spectra of TPPFe^{II}NO taken at (a) 1.8, (b) 21, and (c) 79.8 μs. (Inset) The kinetic profile of photoexcited (7-ns pulse) TPPFe^{II}NO monitored at (inset) 443 nm.

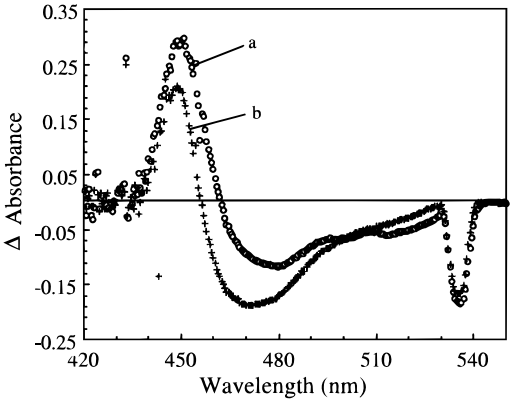

Figure 2. Transient absorption difference spectra of TPPFe^{II}NO taken at (a) 10 and (b) 40 ps. The negative-going signals centered at 532 nm were due to scattered excitation light (532 nm).

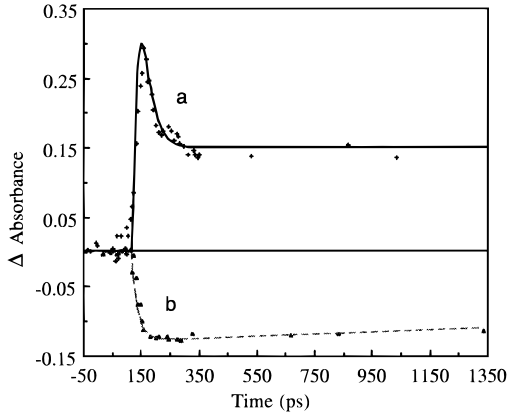

Figure 3. Kinetic profiles of photoexcited (30 ps pulse) TPPFe^{II}NO at (a) 450 and (b) 470 nm.

Results

Direct Excitation Experiments. Earlier we reported a flash photolysis study on TPPCo^{II}NO in benzene at room temperature on time scales from femtoseconds to milliseconds.[18] We deduced therefrom that NO was dissociated from its ligand site within 10^{-12} s of photon absorption. Here we describe similar direct excitation studies on the related species TPPFe^{II}NO. Argon-saturated solutions of TPPFe^{II}NO in benzene ($A_{355nm} \sim 0.4$) at room temperature were exposed to 7-ns pulses at 355 nm with an energy of a few millijoules per pulse. The resulting transient difference spectrum, appearing immediately after the pulse, is shown in Figure 1. Clearly seen are negative absorptions (bleachings) centered at 400 and 469 nm and positive absorption peaks at 425 and 443 nm. This spectrum corresponds to the difference ground state spectrum between TPPFe^{II}NO and TPPFe^{II}, indicating loss of NO.[8] The kinetic profile, monitored at 443 nm (Figure 1 inset), showed second-order kinetic decay to reform the starting material with a bimolecular rate constant of $(5.2 \pm 0.05) \times 10^9$ M^{-1} s^{-1}. These data indicate that NO is ejected from the metal center on time scales shorter than our *ca.* 10 ns time scale, which essentially confirms the conclusions of Hoshino and Kogure.[8] The overall light-induced process can be represented by the following scheme:

$$\text{TPPFe}^{II}\text{NO} \xrightarrow{h\nu} \text{TPPFe}^{II} + \text{NO} \quad (1)$$

$$\text{TPPFe}^{II}\text{NO} \rightarrow \text{TPPFe}^{II}\text{NO} \quad (2)$$

In order to pursue the details of reaction 1, shorter time scale instrumentation was employed. The TPPFe^{II}NO−benzene system was investigated using a 30-ps pulse of 532-nm light coupled with the diode array spectrograph. Figure 2 shows transient absorption spectra recorded at 10 (nominally, i.e., during the excitation pulse) and 40 ps (nominally, i.e., at the conclusion of the excitation pulse). At 40 ps the maximum at 450 nm and the minimum at 470 nm correspond to those spectral features observed at 1.8 μs (Figure 1). Note that there is no information below 440 nm because of minimal light transmission by the highly absorbing sample in this region. Thus, the transient seen to be present at the end of the pulse in the nanosecond studies develops within the risetime of our picosecond system also, showing that denitrosylation occurs at least within a few picoseconds of the light absorption event. Close examination of the transient spectra in Figure 2 shows that there are spectral shifts from 455 to 450 nm and from 478 to 470 nm in the interval between the 10- and 40-ps spectra. The kinetic profiles monitored at 450 and 470 nm reveal interesting differences (Figure 3). The kinetic profile at 450 nm shows an instantaneous rise and a subsequent fast decay, both of which follow the rise and fall of the laser pulse. The decay tends to a nonzero baseline. At 470 nm there is an instantaneous bleaching, which remains for longer than 1400 ps.

In order to examine the early processes involved in denitrosylation, a pump-probe experiment employing a 200 fs excitation pulse at 400 nm was employed. Figure 4 shows the kinetic profile obtained at 450 nm and represents the detail of the first 50 ps of curve (a) in Figure 3. Subsequent to the pulse, there is a rise in absorption (Figure 4, inset) followed by a decay to a nonzero baseline. The total time profile from $t = 0$ to 50 ps shown in Figure 4 could be fitted by a combination of three exponentials. The rise in absorption followed a single exponential with a rate constant of $7.3 \pm 0.4 \times 10^{11}$ s^{-1}; the two exponentials in the decaying region had rate constants of $5.0 \pm 0.3 \times 10^{11}$ and $1.05 \pm 0.05 \times 10^{11}$ s^{-1}. The kinetics at 470 nm were significantly different (Figure 5). There a negative absorption was formed post-pulse with a rate constant of $1.0 \pm 0.05 \times 10^{12}$ s^{-1}. As can be seen, this was preceded by a positive-going signal that decayed with the pulse (inset Figure 5). It may be that more information can be gained using shorter excitation pulses. The rate constant for the growth of the bleach at 470 nm (1.0×10^{12} s^{-1}) is larger than that for the fast decay (5.0×10^{11} s^{-1}) monitored at 450 nm, but not too different from that measured at 450 nm for the growth of the positive signal (7.3×10^{11} s^{-1}).

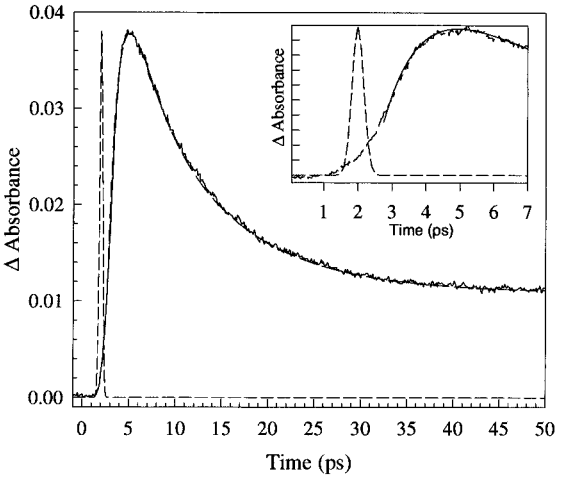

Figure 4. The kinetic profile of photoexcited (200 fs pulse) TPPFe^{II}NO at 450 nm. The dashed signal is the instrument response function (300 fs fwhm). (Inset) The first seven picoseconds of the kinetic profile at 450 nm in the main figure.

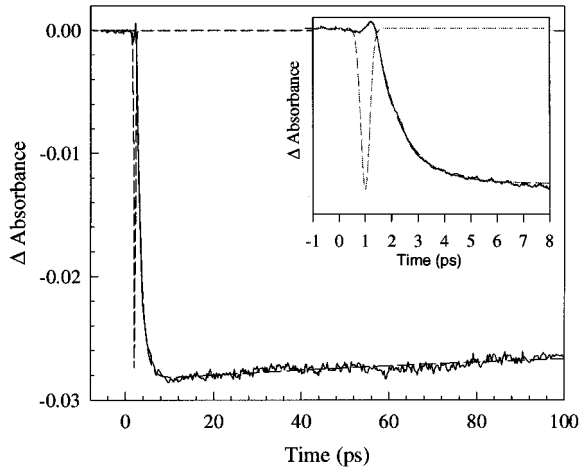

Figure 5. The kinetic profile of photoexcited (200 fs pulse) TPPFe^{II}NO at 470 nm. The dashed signal is the instrument response function (300 fs fwhm). (Inset) The first eight picoseconds of the kinetic profile at 470 nm in the main figure.

Energy Transfer Experiments. Direct excitation by photon absorption in the porphyrin Soret band initially generates π^* states localized on the porphyrin macrocycle which are of the same multiplicity as the starting ground state. An alternative approach for excitation of the nitrosyl metalloporphyrin is by energy transfer from the triplet states of photoexcited donor molecules (sensitizers). The scheme employed is as follows:

Scheme 1

$$S \rightarrow S^* \rightarrow T^*$$
$$T^* + MNO \rightarrow S + MNO^*$$
$$MNO^* \rightarrow ??$$

In this study a variety of triplet sensitizers with well-characterized energies ranging from 7000 to 25000 cm^{-1} were employed. The sensitizer triplets were produced by exciting the sensitizer in argon-saturated benzene solutions with 7 ns pulses of optimal wavelength light. The bimolecular rate constants for energy transfer were determined by monitoring the decay of the triplet of the chosen sensitizer (inset Figure 6) in the presence of a range of acceptor (iron(II) or cobalt(II) nitrosylporphyrin) concentrations. The slope of a plot of observed rate constant for triplet decay versus acceptor concentration yielded the bimolecular rate constant for energy transfer for those particular

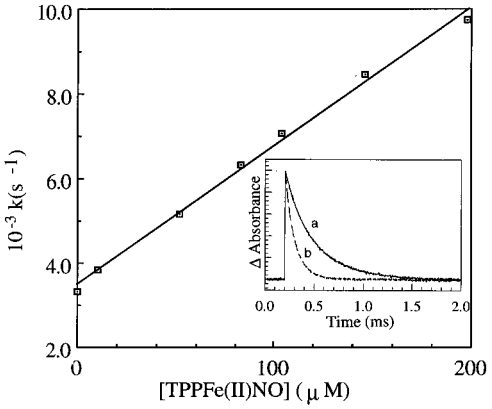

Figure 6. Energy transfer competition plot for TPPFe^{II}NO quenching SiNC triplet in benzene solution. The bimolecular rate constant for energy transfer was determined to be 3.3×10^7 M^{-1} s^{-1}. (Inset) Kinetic profiles, monitored at 595 nm, of SiNC triplet decay (a) in the absence of quencher and (b) in the presence of 198 μM of TPPFe^{II}NO.

Table 1.

sensitizer	triplet energy (cm^{-1})	quenching constant for TPPCo^{II}NO^r	quenching constant for TPPFe^{II}NO^r
benzophenone	24200[g]	8.8×10^9	1.2×10^{10}
phenanthrene	21800[g]	1.4×10^{10}	1.2×10^{10}
pyrene	16930[g]	7.9×10^9	1.2×10^{10}
acridine	15940[g]	9.9×10^9	5.0×10^9
anthracene	14870[g]	9.6×10^9	3.6×10^9
terthiophene[a]	13935[h]	6.4×10^9	4.4×10^9
perylene	12536[i]	4.5×10^9	3.2×10^9
DPOT[b]	11050[j]	6.7×10^9	2.2×10^9
tetracene	10250[g]	5.1×10^9	3.3×10^9
pentacene	8050[k]	1.6×10^9	4.9×10^8
β-carotene	8050[l]	4.1×10^8	4.1×10^8
rubrene	8000[m]	3.1×10^8	
SiPC[c]	8000[n]		2.0×10^8
GePC[d]	7827[o]	3.8×10^7	5.8×10^7
SiNC[e]	7520[p]	1.0×10^7	3.3×10^7
SnNC[f]	7230[q]		4.5×10^8

[a] 2,2′:5′,2″-Terthiophene. [b] 1,8-Diphenyl-1,3,5,7-octatetraene. [c] $(Hex_3SiO)_2$Si-phthalocyanine. [d] $(OSiEt_3)_2$Ge-$(OBu)_8$-phthalocyanine. [e] [SiO(*i*-$C_4H_9)_2$*n*-$C_{18}H_{37}]_2$Si-naphthalocyanine. [f] [SiO(*n*-$C_6H_{13})_3]_2$Sn-naphthalocyanine. [g] See ref 47. [h] See ref 48. [i] See ref 49. [j] See ref 50. [k] See ref 51. [l] Personal communication from Professor Anthony A. Gorman. [m] See ref 52. [n] See ref 53. [o] See ref 54. [p] See ref 55. [q] See ref 56. [r] M^{-1} s^{-1} ± 5%.

reaction partners (Figure 6). The same experimental series was repeated for all the chosen sensitizers. The obtained rate constants and the sensitizer triplet energies are collected in Table 1.

Discussion

The earlier communication from this laboratory focused on the processes involved in the deactivation of the photoexcited TPPCo^{II}NO compound.[18] In that work Scheme 2 was presented

Scheme 2

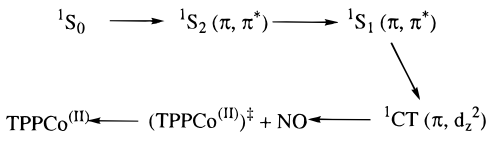

as defining the reactions pursuant to light absorption in TPPCo^{II}NO in benzene solution: where the double dagger indicates a vibrationally excited ground state and the CT state refers to a metal-centered charge transfer state. The deactivation

of S_2 to S_1 was identified as being very rapid, $\tau < 500$ fs. The S_1 state decayed to the CT state with a rate constant of $4.7 \pm 0.2 \times 10^{11}$ s^{-1}; the formation of this CT state was deduced to be the rate-limiting step in the denitrosylation sequence. The NO-free metalloporphyrin was formed in a vibrationally excited ground state which relaxed to $v = 0$ with a rate constant of $9.0 \pm 0.5 \times 10^{10}$ s^{-1}. The ultrafast experiments showed no indication of excited states of the nitroso complex formed by a parallel process to the $S_1 \rightarrow$ CT transition. Thus, each absorbed photon leads to NO loss. Eventually the metalloporphyrin and NO which were generated in the argon-purged solution recombined according to second-order kinetics with a bimolecular rate constant of $7.9 \pm 0.4 \times 10^9$ M^{-1} s^{-1}.

The results presented in this work taken in conjunction with those presented in the earlier communication[18] demonstrate that denitrosylation of both $TPPFe^{II}NO$ and $TPPCo^{II}NO$ occurs on time scales shorter than the time resolution of our picosecond instrumentation. The nanosecond studies indicate that the recombination of the NO and the NO-free metalloporphyrins occurs in a bimolecular, second-order process, under the experimental conditions, on μs to ms time scales (Figure 1) in agreement with the earlier work of Hoshino et al.[8,14]

The results of the ultrafast studies obtained here for the iron analogue can best be discussed with the aid of Scheme 3. Given that the species observed at 50 ps (Figure 4) in the femtosecond study is identical to that seen at post 30 ps (Figure 3) in the picosecond experiments, *viz.*, the thermally relaxed, NO-free porphyrin, and that the lowest-valued rate constant extracted from the kinetic profile at 450 nm (1.05×10^{11} s^{-1}) corresponds to vibrational cooling of the released metalloporphyrin,[35−37] then the other two rate constants evaluated must account for the four processes labeled 1 through 4 in Scheme 3. The deligation

Scheme 3

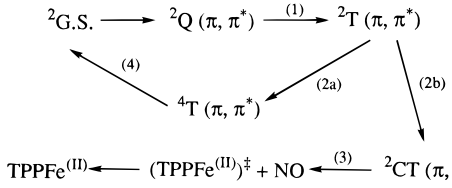

process itself (3), by analogy with the cobalt(II) porphyrin case, is probably very rapid and rate-limited by the formation of the CT state, process 2b. The indication of processes occurring within the pulse in the 470 nm profile (Figure 5 inset) probably indicates that the deactivation of the initially formed upper excited doublet state, ^{2}Q, to yield the lower doublet state, ^{2}T, process 1, happens on time scales shorter than 200 fs. The remaining two rate constants must then describe the remaining two processes: the partitioning of the ^{2}T state into the CT and ^{4}T states (7.3×10^{11} s^{-1}), and the slower deactivation of the ^{4}T state to the ground state (5.0×10^{11} s^{-1}). Thus, in Figure 4 (inset) the species that reaches maximal absorbance near 5 ps is assigned to the ^{4}T(π,π*) state of $TPPFe^{II}NO$. This is supported by a report from Cornelius et al., who observed a transient absorbing at 450 nm and decaying with a lifetime of 50 ps in the photoexcited $TPPFe^{III}Cl$ system which they ascribed to the triplet state.[38] Worth noting here is that the rate parameter $k = 7.3 \times 10^{11}$ s^{-1} describing the quartet state formation rate is actually a composite rate constant involving the rate parameters for reactions 2a and 2b (*v.i.*).

Two reasons present themselves which make it unlikely that NO is lost from the ^{4}T state. The first involves a multiplicity argument. To conserve the spin in the system, for a quartet state to unimolecularly dissociate to yield a doublet (NO), the resulting $TPPFe^{II}$ must be formed in an (excited) triplet state, yet there was no evidence for the existence of such a state in this system. The other reason concerns the differing evolutions of the kinetic profiles at 450 (Figure 4) and 470 nm (Figure 5). The growth of the bleach at 470 nm shows development of the NO-free porphyrin from photoexcited $TPPFe^{II}NO$ with $k = 1.0 \times 10^{12}$ s^{-1}. This is more rapid than the decay of the ^{4}T state as monitored at 450 nm (5.0×10^{11} s^{-1}) and indicates that NO loss does not arise from the decay of the quartet state. In fact, the similarity of the rate constants of 1×10^{12} s^{-1} for the bleach induced at 470 nm and 7.3×10^{11} s^{-1} for the growth of absorption at 450 nm suggests that processes 2a and 2b are together controlling the NO release. Thus, the ^{4}T state and the NO-producing CT state arise as competing processes from the decay of a common precursor, the ^{2}T state. These considerations provide a hint to the explanation of why $\Phi_{(NO)}$ values differ in the Fe and Co porphyrins, of which more later.

The energy transfer experiments were undertaken to gain insight into the nature of excited states of the nitrosyl metalloporphyrins that could not be revealed by the direct excitation method. The approach employed borrows from that originated by Sandros, who demonstrated that the energy level of an energy-accepting state could be evaluated from a series of measurements of bimolecular rate constants for energy transfer from a set of donors of known energy (E_D).[26] The required state energy, E_A, could be obtained from a fit of the equation:

$$k_{ET} = k_d\left[\frac{\exp(-\Delta E/kT)}{1 + \exp(-\Delta E/kT)}\right] \qquad (3)$$

in which $\Delta E = E_A - E_D$, and k_d represents the value of the diffusion-limited rate constant. An extended version of the Sandros equation was employed by Wilkinson et al. in a study of energy transfer involving a series of chromium complexes with a number of accepting states of different multiplicity.[39−43] Following Wilkinson et al., we used the following equation for the Fe(II) complex:

$$k_{ET} = \frac{k_d}{6}\left[\frac{4\exp(-\Delta E^{IV}/kT)}{1 + \exp(-\Delta E^{IV}/kT)} + \frac{2\exp(-\Delta E^{II}/kT)}{1 + \exp(-\Delta E^{II}/kT)}\right] \qquad (4)$$

In this equation the first exponential term refers to the energy transfer to the quartet (trip-doublet) state and $\Delta E^{IV} = E_A{}^{IV} - E_D$; the second term relates to the doublet CT state and $\Delta E^{II} = E_A{}^{II} - E_D$. The pre-exponential multipliers of $^4/_6$ and $^2/_6$ apply because of the combination of the spin-angular momentum terms of a triplet state donor with a doublet ground state acceptor. Thus, in the encounter complex there are a total of six spin sub-states, four quartet and two doublet. Figure 7 shows a plot of the data in Table 1 for $TPPFe^{II}NO$ presented in semilogarithmic form of eq 4 (Sandros type). Two clearly separated plateaus are seen; the upper one ($E > 16200$ cm^{-1}) corresponds to rate constants of 1.2×10^{10} M^{-1} s^{-1}, which equals the

(35) Alden, R. G.; Chaez, M. D.; Ondrias, M. R.; Courtney, S. H.; Friedman, J. M. *J. Am. Chem. Soc.* **1990**, *112*, 3241.
(36) Lingle, R., Jr.; Xu, X.; Zhu, H.; Yu, S. C.; Hopkins, J. B.; Straub, K. D. *J. Am. Chem. Soc.* **1991**, *113*, 3992.
(37) Henry, E. R.; Eaton, W. A.; Hochstrasser, R. M. *Proc. Natl. Acad. Sci. U. S. A.* **1986**, *83*, 8982.
(38) Cornelius, P. A.; Steele, A. W.; Chernoff, D. A.; Hochstrasser, R. M. *Chem. Phys. Lett.* **1981**, *82*, 9.
(39) Wilkinson, F.; Tsiamis, C. *J. Am. Chem. Soc.* **1983**, *105*, 767.
(40) Wilkinson, F.; Tsiamis, C. *J. Chem. Soc., Faraday Trans.* **1981**, *77*, 1681.
(41) Wilkinson, F. *Pure Appl. Chem.* **1975**, *41*, 661.
(42) Wilkinson, F.; Farmilo, A. *J. Chem. Soc., Faraday Trans.* **1976**, *72*, 604.
(43) Wilkinson, F.; Tsiamis, C. *J. Phys. Chem.* **1981**, *85*, 4153.

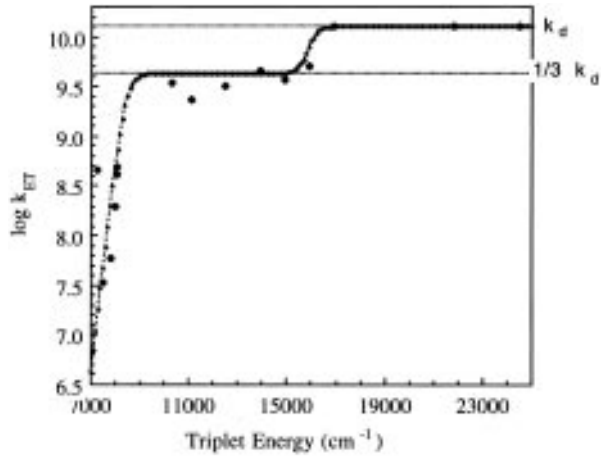

Figure 7. Modified Sandros plot for TPPFe^{II}NO (see text). Fit shows energies of excited states of TPPFe^{II}NO are $E^{IV} = 16200$ cm^{-1} and $E^{II} = 8650$ cm^{-1}.

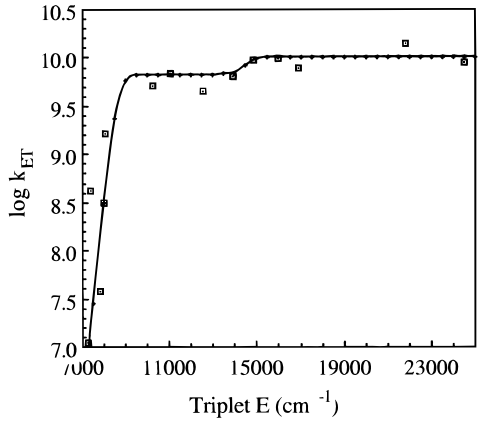

Figure 8. Modified Sandros plot for TPPCo^{II}NO (see text). Fit shows energies of excited states of TPPCo^{II}NO are $E^{III} = 14700$ cm^{-1} and $E^{I} = 8900$ cm^{-1}.

diffusion limit. Here exothermic energy transfer is occurring to the nitrosylporphyrin from donor triplet states having E_D in excess of that of all possible accepting states of the iron complex, whatever their spin nature. The lower plateau (8650 cm^{-1} < E < 16200 cm^{-1}) is near $k = 4 \times 10$ M^{-9} s^{-1}, i.e., $^1/_3$ of k_d. This corresponds to a diffusion and multiplicity-limited reaction between a triplet donor of intermediate energy and a doublet acceptor ($^1/_3$ of all collisions are effective). Along this plateau, quenching to form the doublet state is exothermic and quenching to form the quartet state is endothermic. The fit of eq 4 to the data in Table 1 yields values of $E_A^{IV} = 16200 \pm 800$ cm^{-1} and $E_A^{II} = 8650 \pm 450$ cm^{-1} for the Fe(II) complex. At lower donor triplet energy (*ca.* <8650 cm^{-1}), energy transfer to form both doublets and quartets is endothermic and the rate constants drop off exponentially with donor triplet energy.

The TPPCo^{II}NO complex contains a d-7 metal combined with a doublet NO and is therefore a ground state singlet; yet the Sandros-type plot (Figure 8) shows the double-plateau feature as in the Fe(II) case, and the fit leads to energy values of $E_A^{III} = 14700 \pm 735$ cm^{-1} and $E_A^{I} = 8900 \pm 450$ cm^{-1}. These plateaus are a manifestation of two effects. The first concerns the allowedness of the singlet state formation. Quenching of a triplet excited state by a singlet ground state quencher to form a singlet ground state sensitizer and an excited state singlet quencher is a spin-forbidden reaction. The rate constant for this type of energy transfer process should be less than diffusion controlled, hence the existence of the lower plateau. The other effect concerns the identity of the lower energy state formed from quenching of the excited state triplets. This state is thought to be a charge transfer state of (π, d_z^2) nature. Since it is a charge transfer state involving the internal orbitals of the incorporated metal, it is not unreasonable to assume that access to this buried orbital by the triplet sensitizer is sterically hindered and therefore the rate constant for quenching should be less than diffusion controlled. The magnitude of the lower plateau should be some indication as to the geometric constraints required in the encounter complex to facilitate energy transfer. A similar slight negative deviation from the $^1/_3$ diffusion limit can be seen in the Sandros plot (Figure 7) for TPPFe^{II}NO, reflecting the steric inhibition of the triplet donor in that system.

The energy transfer kinetic studies and the modified Sandros treatment described above lead to the significant conclusion that both nitrosyl porphyrins studied possess triplet (or trip-doublet) and CT states that can be effectively populated by energy transfer and the energies of these states are revealed by the treatment. This allows the construction of the energy-level diagrams presented in Figure 9 for the two nitrosyl complexes. Significant observations emerge from these diagrams: one is that the two CT states have energies that are different by only 250 cm^{-1}. Thus the large differences in the photoinduced deligation yields ($\Phi_{NO} = 1.0$ for TPPCo^{II}NO and $\Phi_{NO} = 0.5$ for TPPFe^{II}NO) in benzene reported by Hoshino and Kogure[8] and confirmed here would appear *not* to be a reflection of the energy of the state responsible for deligation. On the other hand, there is a large difference in the energy gaps that govern intersystem crossing in the two complexes. In the Fe(II) complex this $^2T \rightarrow {}^4T$ gap is 1200 cm^{-1}, whereas the $^1S \rightarrow {}^3T$ gap in the Co(II) complex is 3900 cm^{-1}. This presumably imparts an energy-gap-law type of dependence on the rate constants which enables the intersystem crossing in the Fe(II) system to effectively compete with internal conversion to the CT state. In the Co(II) system the energy gap is much larger, and the intersystem crossing rate constant is too small to effect any serious competition to the internal conversion process. Another possible influence on the intersystem crossing efficiency resides in the fact that the Fe(II) system may be considered as a combination of a localized singlet on the porphyrin and a localized doublet on the Fe^{II}−NO, in which case it is not unreasonable to infer that the unpaired electron in the region of the porphyrin provides an inhomogeneous magnetic field that induces intersystem crossing much as in bimolecular reactions where paramagnetic entities efficiently quench molecular excited states.[44−46] Nitric oxide itself has been shown to be particularly effective in this regard.[44,45]

These considerations lead to the conviction that it is a difference in the partitioning of energy in the upper excited states and not a difference in the absolute magnitude of the energy of

(44) Gijzeman, O. L. J.; Kaufman, F.; Porter, G. *J. Chem. Soc., Faraday Trans.* **1973**, *69*, 727.
(45) Kearns, D. R.; Stone, A. J. *J. Chem. Phys.* **1971**, *55*, 3383.
(46) *Organic Molecular Photophysics*; Birks, J. B., Ed.; Wiley: London, 1975; Vol. 2, pp 552−555.
(47) *Handbook of Photochemistry*; 2nd ed.; Murov, S. L., Carmichael, I., Hug, G. L., Eds.; Marcel Dekker: New York, 1993; pp 4−97.
(48) Evans, C. H.; Scaiano, J. C. *J. Am. Chem. Soc.* **1990**, *112*, 2694.
(49) Monti, S.; Gardini, E.; Bortolus, P.; Amouyal, E. *Chem. Phys. Lett.* **1981**, *77*, 115.
(50) Chattopadhyay, S. K.; Das, P. K.; Hug, G. L. *J. Am. Chem. Soc.* **1982**, *104*, 4507.
(51) Hall, G. C. *Proc. R. Soc. A* **1952**, *213*, 113.
(52) Dreeskamp, H.; Koch, E.; Zander, M. *Ber. Bunsenges. Phys. Chem.* **1974**, *78*, 1328.
(53) Wheeler, B. L.; Nagasubramanian, G.; Bard, A. J.; Schechtman, L. A.; Dininny, D. R.; Kenney, M. E. *J. Am. Chem. Soc.* **1984**, *106*, 7404.
(54) Rihter, B. D.; Kenney, M. E.; Ford, W. E.; Rodgers, M. A. J. *J. Am. Chem. Soc.* **1990**, *112*, 8064.
(55) Firey, P. A.; Ford, W. E.; Sounik, J. R.; Kenney, M. E.; Rodgers, M. A. J. *J. Am. Chem. Soc.* **1988**, *110*, 7626.

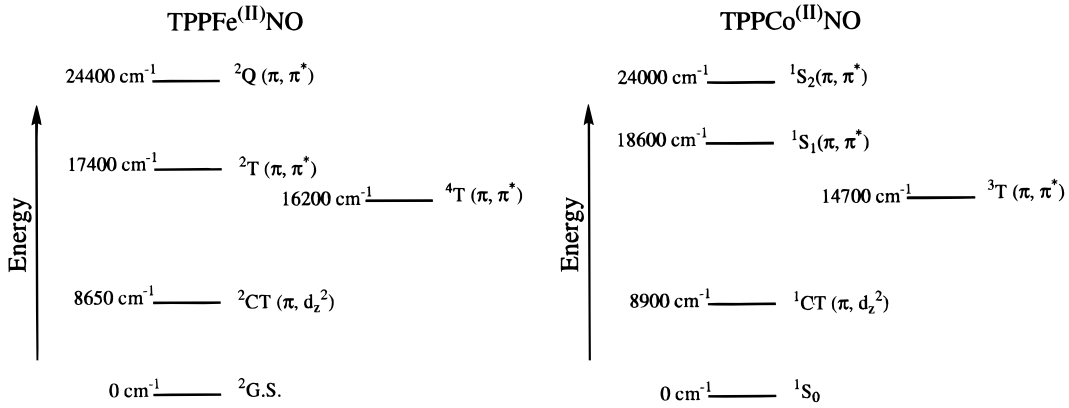

Figure 9. Proposed state energy diagrams for $TPPFe^{II}NO$ and $TPPCo^{II}NO$.

the NO-releasing state that is responsible for determining the quantum efficiency of NO loss from the photoexcited nitrosyl metalloporphyrins. The other major conclusion from this study is that the rate at which the CT states release NO is too fast to measure and is determined by the rate at which the state is populated from the upper reaches of the manifold. All that can be said is that the M−NO bond dissociates in less than 10^{-12} s after the dissociative state is formed, presumably within the first vibration. Because of the rate-limited property of this process, this is not a question that can be resolved by employing even shorter excitation pulses. Finally, since the ^{4}T state in the Fe(II) complex is formed with a rate constant of 7.3×10^{11} s^{-1} and this is the composite of two processes of equal efficiency, then the intersystem crossing process alone has a rate constant of some 3.6×10^{11} s^{-1}. It is of interest to contemplate that even reactions that proceed in a few picoseconds or less can find themselves in competition, and that even the most rapid processes have effects that have significance on the human time scale.

Acknowledgment. The femtosecond studies reported herein were performed at the Chemistry Department at the University of Michigan (Ann Arbor). We would like to thank Roseanne Sension and Larry Walker II for access and for assistance with the experiments. E.A.M. would like to thank the Graduate College of Bowling Green State University and the Helen and Harold McMaster Foundation for fellowship support throughout this work. This work was supported in part by the Center for Photochemical Sciences at Bowling Green State University.

JA962510S

(56) (a) Ford, W. E.; Rihter, B. D.; Rodgers, M. A. J.; Kenney, M. E. *J. Am. Chem. Soc.* **1989**, *111*, 2362. (b) Ford, W. E.; Rodgers, M. A. J.; Schechtman, L. A.; Sounik, J. R.; Rihter, B. D.; Kenney, M. E. *Inorg. Chem.* **1992**, *31*, 3371.